| OF |
AD
A057067

END
DATE
FILMED
9-78
DDC

LEVEL II

# von KARMAN INSTITUTE

①

FOR FLUID DYNAMICS

TECHNICAL NOTE 126

FILM COOLING AND END WALL HEAT TRANSFER

IN SMALL TURBINE BLADE PASSAGES

D D C

RECEIVED

AUG 4 1978

E
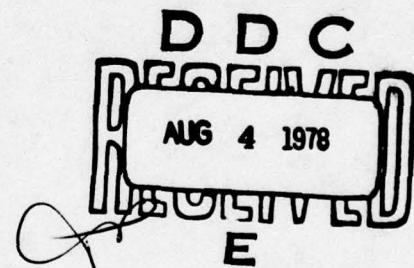
J.-P. VILLE, M. GODARD, B.E. RICHARDS, C. SIEVERDING

FEBRUARY 1978

RHODE SAINT GENESE BELGIUM

78 07 31 100

VON KARMAN INSTITUTE FOR FLUID DYNAMICS

TECHNICAL NOTE 126

(14) VKI-TN-126

(9) Annual rept. Jul. 76 - Dec 77,

(6) FILM COOLING AND END WALL HEAT TRANSFER
IN SMALL TURBINE BLADE PASSAGES,

(10) J.-P. VILLE, M. GODARD, B.E. RICHARDS, C. SIEVERDING

(15) DA-ERO-75-G-074

(16) 1T161142B35E (17) 4P

(11) FEB 978 (12) 51 p.

367 475
78 07 31 100

TABLE OF CONTENTS

ACKNOWLEDGEMENTS

ABSTRACT

Two topics have been studied related to the cooling of the end wall of a turbine passage. The first concerns the development of a method for measuring the adiabatic wall effectiveness and heat transfer coefficient of a film cooling system for protecting a surface from high heating derived from a hot compressible flow. The second concerns the measurement of the heat transfer rate distribution to a turbine cascade end wall in order to choose an appropriate film cooling system. These are related to providing the background to the final phase of the study in which the effectiveness of a film cooling system to cool a turbine end wall will be made, combined with the measurement of the aerodynamic losses incurred by such a system.

LIST OF SYMBOLS

d	coolant hole diameter
h	heat transfer coefficient of films in terms of $(T_{rm}-T_{wo})$ (see eq. 6)
h_f	heat transfer coefficient of film (eq.1)
h_o	heat transfer coefficient on outside wall with film cooling (eq .2)
m	coolant mass ratio, $\rho_c u_c / \rho_m u_m$
M	Mach number
p	pressure
q	heat transfer rate
Re	Reynolds number
T	temperature
u	velocity
x	distance along surface
η	adiabatic wall effectiveness (eq . 3)
Θ	non-dimension coolant temperature parameter (eq.5)
ρ	density of fluid

SUBSCRIPTS

aw	adiabatic wall
c	coolant
f	film
i	injection
m	mainstream
o	supply condition or without injection
r	recovery
w	wall
∞	static condition

LIST OF FIGURES

INTRODUCTION

Film cooling is increasingly being used to protect heated components in advanced gas turbine engines used in aerospace applications. For manufacturing and strength reasons, the injection of coolant onto the surface is usually through a grouping of inclined holes. In the region near the wall downstream of injection when the film is most effective in protecting the blade surface the flow behaviour is dominated by three-dimensional effects mainly of a viscous nature. In applying cooling to surfaces in passages between blades in small gas turbines, the flow is further complicated by the three-dimensional behaviour associated with the existence of pronounced secondary flows. The resulting situation is such that at present it is necessary to place most reliance on experimentally based empirical relations to provide information for designers.

The majority of fundamental research studies on film cooling have been carried out under incompressible flow situations (ref.1) and a large proportion of these have been in slot cooling. Such studies provide the fundamental bases for prediction methods empirical or otherwise, however accuracy in calculating real turbine flows can only be expected to be achieved under more realistically simulated conditions. Blow down tunnels have been used to provide both Mach number and Reynolds number simulation (ref. 2) but the temperature field simulation has sometimes been ignored. More recently, short duration wind tunnels have been applied to the turbine film cooling problem to provide more appropriate temperature field scaling (e.g,ref.3 & 4)

The work involved in this research is related to studies carried out in piston driven short duration tunnels on the heat transfer to surfaces in an inlet guide vane passage and the effect of film cooling such a passage. The first part of the study, reported in ref. 5, was concerned with the examination of the effect of wall curvature, pressure gradient, Mach number, Reynolds number and flow temperature on film cooling effectiveness in two-dimensional flow situations.

The isothermal wall effectiveness parameter $(1 - q_c/q_0)$ was used to analize the results. It was discussed that the usefulness of the data however could be extended by determining an "adiabatic" film cooling effectiveness derived from experiments carried out with different coolant temperatures. The development and use of this technique in the small compression tube CT-1 is described in the present report. Reported in the second part of this report are the measurements of heat transfer on the end wall of a cascade of vanes typical of that in an advanced turbine. These studies provide the ingredients to the final years study of the measurement of film cooling effectiveness in regions of secondary flow.

PART 1 - FILM COOLING OF A TWO-DIMENSIONAL SURFACE

1. DISCUSSION OF FILM COOLING EFFECTIVENESS

The heat transfer at a particular position on a film cooled turbine blade is usually represented by the equation :

$$q_f = h_f (T_{aw} - T_w) \qquad (1)$$

where T_{aw} is the adiabatic wall temperature of the flow (closely related to the local temperature of the film) and h_f is the associated heat transfer coefficient which has a value not too far different from that without film cooling in a flow with mainstream recovery temperature, T_m, given in the relation :

$$q_0 = h_0 (T_m - T_w) \qquad (2)$$

The adiabatic wall temperature T_{aw}, is normally defined in terms of the film cooling adiabatic wall effectiveness parameter, η given by :

$$\eta = \frac{T_{rm} - T_{aw}}{T_{rm} - T_{rc}} \qquad (3)$$

where T_{rc} is the recovery temperature of the coolant.
In design work; the heat transfer rate is normally determined from values of η and h_f (available from experiments, empirical relationships or predictive techniques), using the relationship :

$$q_f = h_f (T_{rm} - T_w) (1 - \eta \theta) \qquad (4)$$

where θ is a compressible flow version of the non-dimensional parameter first introduced by Metzger et al (ref. 6) defining the level of the coolant temperature with respect to the wall temperature in terms of the mainstream temperature :i.e

$$\theta = \frac{T_{rm} - T_{rc}}{T_{rm} - T_w} \qquad (5)$$

- 4 -

In order to avoid the difficulty of dealing with the adiabatic wall temperature, an alternative relation to eq.1 is :

$$q_f = h (T_{rm} - T_w) \qquad (6)$$

In this relation the only parameter that can reflect the behaviour of the coolant temperature is this newly defined heat transfer coefficient h. Its effect can be seen by combining eqs.(6)and(4),i.e.:

$$h = h_f (1 - \eta\theta) \qquad (7)$$

which equation is plotted in fig.1 with the heat transfer coefficients non-dimensionalized by dividing by h_0. Then h_f and η can be determined from the measurement of the heat transfer coefficient h at two values of θ, i.e.:

$$h_1 = h_f (1 - \eta\theta_1)$$

$$h_2 = h_f (1 - \eta\theta_2) \qquad (8)$$

$$\text{where } \eta = \frac{1}{\theta_{h=0}} = \frac{h_2 - h_1}{h_2\theta_1 - h_1\theta_2} \qquad (9)$$

$$\text{and } h_f = h_{\theta=0} = \frac{h_2\theta_1 - h_1\theta_2}{\theta_1 - \theta_2} \qquad (10)$$

The assumption of linearity of the temperature field, implied in eqs.(1),(2) and (6), should be examined for the design case in which total, wall and coolant temperature may be at levels of the order of 2000 K, 1200 K and 600 K respectively for a future projected turbine. The fluid temperature and hence the gas density gradient are so high as to suspect the accuracy of an assumption concerning a constant property fluid even though the flow Mach number may be small and experiments are necessary to examine the implications of this. However, the achievement of linearity in the relationship h $\sim$ θ is not essential as long as measurements are made in the θ range of interest. This range is normally from 1.25 to 1.75 for aircraft propulsion units.

In such a situation an assumption of linearity can be used to approximate the results to get appropriate values of h_f and η by extrapolation, used together to determine h of q_f in the region of interest, the original measurement accuracy will be realized in a design calculation.

2. EXPERIMENTAL EQUIPMENT FOR FILM COOLING STUDY.

2.1 The isentropic light piston tunnel CT1

The VKI isentropic light piston tunnel (ILPT) CT1 is used for this part of the study (fig. 2) The test gas contained in a 3.25m long 102mm diameter tube is compressed and heated isentropically by a 60g free running nylon piston driven by gas entering from a 40 atm pressure reservoir. When the gas achieves the pre-designated pressure and hence temperature, a fast operating shutter valve is opened in 4msec allowing the test gas to flow through the test section. The volumetric flow of the gas entering the tube from the reservoir and the gas leaving the tube through the test section are matched so that, the pressure and flow conditions remain constant until the piston reaches the end of the tube. The tube pressure then continues to rise until the incoming gas flow is stopped. In the test section, pressure and temperature follow a steplike variation which is most suitable for the application of a transient heat transfer measurement.

The test section used in this study has typically a throat area of 1.5cm^2 with a rectangular channel and is connected to a dump tank having a volume equivalent to the volume of the tube. Subsonic operation is achieved by using a throat downstream of the test section. The dump tank pressure is kept low enough to keep the main flow sonic through this throat during a test. Before firing, the tube is set to the desired initial pressure. After presetting the instrumentation, the tunnel is set into operation by opening quickly a manually operated ball value. The compression lasts about 1 sec and the test duration 0.1 sec After a test the system is brought to room pressure, the piston reset at the end of the tube ready for the next test.

2.2. Secondary gas supply

For film cooling experiments, the secondary gas (air) is taken from a 50 litre reservoir precharged at a pressure up to 35 atm at room temperature. The temperature is adjusted to the desired level as the gas passes through a small regenerative heat exchanger and the mass flow controlled by a choked calibrated orifice close to the test section. A pneumatically operated ball valve then initiates the gas injection into the test section (fig.3).

The heat exchanger is made of a stack of brass gauze screen matrices in a 25 mm diameter and 40 cm long steel tube. It has been designed to heat or cool the secondary gas at the maximum coolant mass flow rate with a temperature variation of less than 1% during the test with minimum pressure losses. The heat exchanger temperature can be adjusted between -40° and +120°C by a low pressure secondary open loop system using an electrical heater or a cooler made of an alcohol bath whose temperature can be decreased down to -70° by addition of dry ice. After a few minutes of heating or cooling, when the required temperature is reached, the heat exchanger is isolated from the low pressure loop and connected to the high pressure reservoir ready for a test.

The calibrated orifice has been placed after the heat exchanger to minimise the volume between itself and the test section : the coolant pressure can then adjust itself to the main flow pressure and follow even a very small pressure fluctuation within a delay of one or two msec giving a nearly constant mass flow rate into the test section during the test. This is particularly important for small injection rates when coolant pressure is very close to main flow static pressure.

2.3 Instrumentation

All the pressures in the tube, the test section and secondary gas supply are measured with Validyne variable reluctance diaphragm transducers, the response time of these transducers being compatible with the relatively slow pressure variations during the test.

Heat transfer rates are measured, using a transient surface temperature technique, with standard thin film platinum resistance thermometers, brush painted and fired on quartz inserts associated with appropriately designed analogue circuits (ref.7)

Main flow temperature was measured in a test series prior to the present one with a fine tungsten wire probe used as an equilibrium temperature probe. The temperature is assessed from the change in resistivity of the wire during the test and this is corrected for conduction end losses to the wire support (ref. 8). Response times of less than 1 msec are achieved. This rapid response time enabled subtle variations in temperature to be easily detected.

For film cooling tests, the temperature of the secondary flow is measured at 2 points inside of the heat exchanger, upstream of the flow meter and in the small settling chamber just before the injection holes, using thermocouples made with 0.1 mm diameter chromel alumel wires. The reponse time was found to be of the order of 20 msec. This slow response is due to very low gas velocity at various measurement points. Coolant pressure is also measured before the calibrated orifice and in the injection chamber.

Oscilloscopes and an u.v. oscillograph with a speed up to 256 cm/sec fitted with galvanometers with response times up to 5 kHz are used for recording the signals from system sensivity and facilitate the calibration.

During operation, the various events are synchronised
by a trigger and delay unit. A first triggering pulse is set off
from the achievement of a "threshold voltage" by the processed
signal from the transducer monitoring the tube pressure. This
pulse is used to activate the valve to initiate injection and to
start the u.v. recorder and, after an adjustable delay to trigger
the single trace of the oscilloscopes. A second pulse, triggered
in the same way as the first, activates the acturator of the fast
operating shutter valve initiating the flow in the test section.
The injection valve is closed and the recorder is stopped auto-
matically after a suitable time lag to encompass the tunnel
running time.

2.4 The model

The film cooled test surface is one wall of the 13.4 x
15.7 mm rectangular test channel of CT1. Typically, downstream
(and on the centre line of the plate) of an injection section,
10 thin film platinum resistance gauges (with dimension of 4 mm
span by 0.5 mm chord) are positioned within a length of 55 mm.
These gauges average the spanwise heat transfer rate distribution
across 3-4 injection holes. Only several of the gauges were
selected for use in this test programme. A two dimensional span-
wise slot facing upstream is installed on the test surface 30 mm
upstream of the injection position to act as a boundary layer
bleed. The Mach number in the test section is fixed at 0.6 by
a sonic throat of suitable area downstream of the instrumented
plate.

The geometry of the coolant injection was selected as
follows :

hole diameter, d	0.5 mm
spanwise spacing	1.0 mm
number of rows	2
spacing between rows	1.5 mm
injection angle	30°
injection channel length	4 mm
number of holes	25

The nominal conditions selected for study were :

Mach number   0.6
P_{om} 3.0 bar (absolute)
T_{om} 382 K
T_{oc} 267-365 K (T_{is} = 401 K)
T_w ≃ 293 K
Re   2.44 10^7/m

A drawing of the test model is given in fig. 4.

3. EXPERIMENTAL RESULTS

3.1 Description of data recorded from tests

The main flow temperature measurements indicate that this temperatutre varies according to that expected from the measured pressure variations but 5% below the isentropic temperature at the selected measurement time.

Preliminary tests with injection have shown that the secondary flow temperature was not constant during the test as illustrated by the relevant trace for the case of coolant at ambient temperature in Fig. 5. Injection is initiated about 100 msecs before the test to be sure that the air initially between the heat exchanger and the test section is blown out when the main flow starts. As the coolant mass flow is kept constant by the choked orifice, the pressure in the injection settling chamber (again illustrated in Fig. 5) increases to its stable condition for the particular pre-test pressure in the test section. This compression is associated with a temperature rise of the order of 20°C. When the main flow starts, the settling chamber pressure suddenly rises to its nominal value controlled by the test section pressure causing a second increase of pressure and hence of temperature of the secondary gas. These "hot" gases appear to be evacuated after 20 to 30 msec for all coolant temperatures tested. To avoid taking measurements in these unstable periods; it was decided to measure heat transfer and wall temperature 32 msec after the beginning of the test.

This time was also selected because the main flow pressure at that time is then equal to its mean value (nominal) (fig.5). On the typical record presented in fig.5 the coolant temperature variations (T_i) are smoothed because of the relatively poor response time of the thermocouple. The preliminary tests also indicate that the flow conditions upstream of the calibrated orifices were nearly constant during the test (about 0.05% change in pressure and less than 1% change in temperature). Furthermore, the pressure losses through the heat exchanger and valve were found to be negligible. In later tests pressure was then set to the required level in the H.P. reservoir and was measured only before the test. The time dependent temperature however, was measured at the same time as other parameters in all tests as illustrated in fig. 5.

3.2 Data reduction

The secondary mass flow was calculated from the area of the calibrated orifice, A^*, and the upstream flow conditions by the simple formula

$$\dot{m}_i = \beta \times \rho_{oi} \times a_{oi} \times A^*$$

where the density ρ_{oi} and speed of sound a_{oi} are defined from the measurements of P_{oi} and T_{oi}. The mass flux ratio was then obtained from this mass flow, the main flow static conditions and the injection cross sectional area A_i from :

$$m = \frac{\rho_{\infty c} V_c}{\rho_{\infty m} V_m} = \frac{\dot{m}_i}{A_i} \times \frac{1}{\rho_{\infty m} V_m}$$

The wall temperature T_w was obtained from the electrical resistance variations of the gauge and heat transfer q from the output of the analogue circuits by an appropriate calibration of the analogue, the measured temperature coefficient of resistance of the gauge and the thermal properties of the quartz of which the gauge is painted. Heat transfer coefficient is then simply defined by $h = q/(T_{om} - T_w)$ with and without film cooling.

The results were presented at the ratio of the measured heat transfer coefficients with and without injection, h/h_o. This presentation of the results eliminates the possible small systematic error on q that may not be fully eliminated by calibration.

3.3 Results and discussion.

The results of the measurements of h/h_o are first plotted against the mass velocity ratio m for a given injection temperature and the various positions selected. An example is given in fig. 6. Such a graph allows a rapid preliminary check of the results and is used to smooth the curves and to interpolate h/h_o to the desired value of m. The parameter θ is calculated, for each point, from the measured values of T_w, T_i and the main flow temperature assessed from the isentropic temperature $T_{o\,is}$. As carried out for h/h_o, θ is interpolated to the selected m when necessary. Finally, the value of h/h_o obtained by this way for a given mass velocity ratio and various secondary flow temperatures are plotted against θ .

The tests already performed with this technique for four injection temperatures give fairly good results even for "lift-off" conditions as illustrated in fig.7. The straight lines drawn through the experimental points are extrapolated to the θ = 0 and h/h_o = 0 axes giving the values of respectively h_f/h_o and θ = $1/n$ The trend observed seems to be normal,i.e, decreases with the distance and increases with the mass velocity ratio, and close to injection holes (x/d = 7) h_f/h_o increase with m. Complete results of h_f/h_o and (1/θ_o) obtained by this method for x/d = 7 are plotted against m in fig.8. The effective‧ ness 1/θ increases continuously with m up to 83% for m = 0.9 and is nearly constant for m > 1.0, indicating that the lift off occurs for m $\simeq$ 0.9. This lift off condition is also marked by a rapid and continuous increase of h_f/h_o for m > 1. A similar trend was observed by Eriksen and Goldstein (ref.9) but for nearly incompressible flow conditions.

- 14 -

These few results show that this method, is capable of providing useful measurements of film cooling effectiveness and heat transfer coefficient to the designer. The substantial difficulty of altering the coolant temperature is offset by the broadened utility of the data.

4. CONCLUSION

A short duration facility has been used to provide an
assessment of adiabatic wall effectiveness of a film cooling
system with the associated heat transfer coefficient instead of
simple isothermal film cooling effectiveness as usual in short
duration testing. These results were obtained by operating the
experiments under different coolant temperature conditions.
The reliability and repeatability of heat transfer and temperature
measurement is found to be good and the hypothesis of a linear
relationship between a heat transfer coefficient h and a non-
dimensional coolant temperature θ , leading to the evaluation of
adiabatic film effectiveness and classical heat transfer coefficient
is proved experimentally. The modification of the coolant
temperature, introduced complications to the normal simple techniques
associated with short duration testing, but the extra effort
enhanced substantially the value of these measurements taken under
well simulated gas turbine flow conditions.

PART 2 - HEAT TRANSFER ON END WALL OF CASCADE

1. INTRODUCTORY COMMENTS

There exists very little information on the heating distribution on the end wall of a cascade.The only work found in the literature was that of Blair (ref.10) taken in a channel resembling the flow through a cascade. This part of the study was undertaken to generate heat transfer data sufficiently detailed to select a suitable film cooling system.

2. <u>EXPERIMENTAL EQUIPMENT FOR END WALL</u>
<u>HEAT TRANSFER STUDY</u>

2.1 <u>The VKI hot cascade facility CT2</u>

The VKI hot cascade facility CT2 is a scaled up version
of the CT1 facility described in the earlier section (Fig. 9).
The tube is 1 meter in diameter and 5 meters long and designed
to withstand pressures up to 40 atm. The piston, having an
aluminium skirt and a honeycomb face, weighs 27 kg. The tube
is connected to the main Institute 250 bar air supply through 3
in D tubing and its operation initiated by means of a pneumatic-
ally operated ball valve. The heated test flow is released from
the tube into the 25 cm x 10 cm test section by a 20 cm x 10 cm
pneumatically operated gate valve, which through the use of an
exploding detonator opens in a time of the order of 20-30 msec.
A dump tank of approximately 5 m³ volume is situated downstream
of the test section. The test model can either be a cascade of
blades or a channel, the latter used to study fundamental two
dimensional flow fields associated with heated turbine components.

The pressure upstream of the cascade can be varied
in the nominal range from 0.5 to 7 bars absolute. The pressure
downstream of the cascade can be preset to pressures between
0.1 and 5 bars in order to vary the outlet Mach number and,
with appropriate changes in upstream pressure, Reynolds number.
The temperature can be varied from 290 K to 600 K by appropriate
selection of the initial setting of the tunnel. The model is at
ambient temperature at the beginning of the test and its tempe-
rature changes very little with time.

2.2 Cascade model

The two dimensional blade shape selected for study was one suitable for a high temperature engine application. The profiles for the hub section of a stator blade designed by NASA as in ref. 11 was used. The dimensionless coordinates are given in Fig. 10. The cascade geometry was as follows :

chord length	$c = 60$ mm
pitch	$g = 43.5$ mm
stagger angle	$\gamma = -42°5$
blade height	$h = 100$ mm
inlet air angle	$\beta_1 = 0°$

6 blades giving 5 passages.

The selection of 6 blades was made to ensure periodicity in these quantitative experiments. The model is illustrated in Fig. 11. The end walls on two passages were equipped with thin film platinum resistance sensors. Due to the small pitch and because of the expected severe heat transfer gradients in some regions of the passage, it was necessary to make sufficiently small gauges to ensure a high spatial resolution. However, since the construction of the heat sensors is largely manual and hence time consuming, the number of gauges had to be minimized. The solution was to place the gauges on the ground of polished ends of pyrex rods of 3.2 mm diameter and to fix them on two circular discs of perspex of the same diameter which could turn in the cascade wall to traverse as large and area of the passage as possible. The gauges were positioned and the discs changeable in order to explore a wide range of radial and circumferential positions, while using only 17 sensors. Pressure taps were placed upstream and downstream of the cascade on the side wall in order to measure the Mach number at these positions.

2.3 Test conditions

Since the model is a large one, and the dump tank is
of limited size, the pressure in the dump tank will rise during
a test with an accompanying decrease in Mach number.
In order to keep the Mach number changes as low as possible during
a test it was decided to keep the dump tank vented to atmosphere.
The initial pressure in the tube was selected to be 0.69 bar and
the shutter opened at 1.83 bar giving a temperature increase during
compression from ambient temperature (approximately 295K) to 390K.
The tube pressure, and static inlet and outlet pressures were
measured during the test with Validyne transducers. Once the flows
established, low pressure fluctuations (of 2% of the mean value)
were measured giving resulting Mach number fluctuations of 5%.
The mean measured upstream and downstream pressures were 1.76 bar
and 1.14 bar giving corresponding inlet and outlet Mach numbers
of 0.24 and 0.85. The resulting Reynolds numbers, based on the
chord were repectively $Re_{M_1,c} = 0.40 \times 10^6$ and $Re_{M_2is,c} = 1.08 \times 10^6$.

For these test conditions, the test time was of the
order of 850 msecs, the shutter (when correctly opening such that
it does not rebound) opening time was 20 msec and the flow was
completely established after 40 msecs. Since the performance of
the analogue circuits of the heat transfer sensing equipment does
not extend beyond 60 msecs, the measurements were made after 50 msecs.
The repeatability of the measurements was simply checked by
monitoring the signals from the gauges fixed at the centres of the
two rotating pieces in all tests.

3. RESULTS AND DISCUSSION

3.1 Oil flow visualization

The surface flow on the sidewall was visualized using
an oil dot technique. This method was chosen instead of the oil
visualization method in which a film of oil is placed over the
surface because of the short running time. The technique is to
put small drops of oil forming a mesh on the surface of interest.
The drops then flow in the direction of surface shear during the
testing time leaving trails indicating the path of the dot.
The size of the drops is kept such that they are small relative
to the incoming boundary layer thickness, but large enough to
travel a reasonable distance during the running time. The starting
flow is considered to be of such duration that the drops do not
move substantially until the establishement of the steady flow.
If the drops are kept of constant size, the length of trail can
give a rough idea as to the level of the local shear. The method,
as used in this facility, has not been examined in detail and hence
the final result as shown in fig.12 should be considered as tentative.

3.2 Heat transfer measurements

More than 100 heat transfer measurements were recorded
during the test series. The repeatability was found to be very
good. The unfiltered heat transfer signals reflected the turbulent
nature of the flow, the sidewall boundary layer having developed
from the inlet of the cascade, by showing quite large high frequency
fluctuations.

From the point measurements, constant heat transfer
lines were plotted and presented in fig.13. It can be seen that
the coverage was complete, except for a small region near the half
chord position on the suction surface of the blade. The plot was
made up from results measured in two adjoining passages in which
the periodicity was achieved by comparing measurements at identical
locations within the channels.

The general measurement trends show gradients perpen-
dicular to the flow near the entry to the blading as expected and
gradients near the blade surfaces and near the exit of the blading
parallel to the flow direction indicative of secondary flow
behaviour. A more detailed discussion of the results is made after
the prediction of the sidewall heat transfer as outlined in the
next section.

3.3 Heat transfer prediction

In this preliminary study the heat transfer was predicted
by applying a flat plate empirical method along streamlines with
the Mach number distribution calculated using a potential flow
calculation. The limitations of this method are well recognized,
but the resulting calculations illuminate some characteristics of
the measurements.

Martensen's method as extended by Van den Braembussche
(ref.12) to take into account compressibility effects was used to
predict the potential flow in the passages. The positions of the
streamlines and the calculated Mach numbers are plotted in fig.14.
The suction and pressure side Mach numbers are plotted in fig.15.

The semi-empirical method of Spalding and Chi (ref.13)
was applied along each streamline in turn assuming that the
boundary layer was turbulent from 1 m upstream of the blade row.
Prediction of the heat transfer in this way ignores the secondary
flow effects, the curvature of the flow in a cross-wise manner
and the effect of pressure gradient. The theory had however shown
to give good prediction of two dimensional flows with small pressure
gradients at similar conditions to the present experiment (ref.14)
The wall temperature taken for this calculation was 309 K, a value
typical of that measured after 50msec of test flow duration. The
constant heat transfer lines resulting from this calculation are
plotted in fig. 16.

3.4 Discussion of results

The general level and trend of measured heat transfer
rate is well predicted by the Spalding and Chi technique upstream
of and in the early regions of the passage. Near the exit of the
blading, the trends are poorly predicted and heat transfer rates
of up to 40 per cent greater than and 30 per cent less than pre-
dicted are seen in different regions.

Between the blades and on the level with their leading
edges lies a region of low heat transfer rate ($\sim$ 1.7 w/cm^2).
This is in accordance with the measurements of Blair (ref.9) who
however attributed this to the presence of laminar and transitional
flows, which could not be said of this present experiment.
We credit this phenomena to slowing down of the flow in this region
due to induced effects from the secondary flow behaviour. It can
be seen from the flow visualization pictures that,in this region
there already exists a considerable cross flow.

Low heat transfer rates are also encountered at around
15% chord upstream of the leading edge. This corresponds to the
separation point of the inlet boundary layer seen in fig.12 and
which is at the origin of the horse-shoe vortex formed around such
blunt bodies position on a flat surface. The high heating down-
stream of the leading edge on the suction surface can be attributed
mainly to the rapid increase in Mach number in this region as
demonstrated in fig.14. This high heating is not evident on the
pressure surface due to the low energy fluid associated with the
pressure side passage vortex.

In the passage the heat transfer rate increases as
expected due to the increasing Mach number and at about one third
of the chord there commence large pitchwise heat transfer gradients
which can be attributed to secondary flows. The primary effect of
the secondary flow behaviour is for the low energy and low
temperature flow adjacent to the surface to be swept away exposing
the surface to the higher energy flow resulting in enhanced heating
rates.

The region of low heating rate adjacent to the downstream suction surface coincides with the accumulation and subsequent separation due to the presence of the blade, of this low energy fluid. Low readings of heat transfer were also recorded in a small region near the trailing edge pressure side surface. The reason for this is a little more obscure but it is suggestive of a separation zone associated with the influence of the trailing edge.

More realistic prediction of the heat transfer rates on endwalls can hence only be brought about using more sophisticated analyses. Dodge (ref.15) has obtained a good agreement with the results of Blair (ref.9) by solving the complete Navier Stokes solution . Less labouriously the present method could be refined by applying Spalding-Chi's method on the limiting streamlines obtained from Johnston's triangular model (ref.15) or Kenny's method (ref. 17).

4. CONCLUSIONS

A preliminary study of the heat transfer distribution
to tne end wall of a turbine cascade has been made with a view to
designing an appropriate film cooling system.
Generally upstream of the half chord position, the heat gradients
are parallel to the flow stream and the heat transfer rates can
be reasonably well predicted by simple two-dimensional theories.
Further downstream the heat gradients tend to be perpendicular
to the flow direction indicating the presence of secondary flows.
Values of heat transfer rate up to 40 per cent greater than and
30 per cent less than predicted by two dimensional theory are seen.

REFERENCES

1. GOLDSTEIN R.J. : "Film Cooling", Advances in Heat Transfer, Vol.7; Academic Press, New York, London 1971.

2. LIESS C. : "Film cooling with injection from a row of inclined circular holes - an experimental study for the application to gas turbine blades" VKI TN 97, March 1973.

3. JONES T.V., SCHULTZ D.L.: "Film cooling studies in subsonic and supersonic flows using a shock tunnel" 8th international shock tube symposium, Imperial College, London, July 1971.

4. LOUIS J.F., DERMERJIAN A.M., GOULIOS G.N., TOPPING R.F., WIEDHOPF J.M. : "Short duration studies of turbine heat transfer and film cooling effectiveness" ASME 74-GT-131, April 1974.

5. RICHARDS B.E., VILLE J.P., APPELS C. : "Film cooled small turbine blade research- Film cooling effectiveness at simulated turbines conditions" VKI TN 120, June 1976.

6. METZGER D.E., CARPER H.J. and SWANK L.R.: "Heat transfer with film cooling near non-tangential injection slots" ASME Transactions, J.of Eng. Power, 1968, pp.157-163.

7. SCHULTZ D.L. and JONES T.V. : "Heat transfer measurements in short duration hypersonic facilities" AGARDograph 165, 1973.

8. BACKX E. : "The total temperature in the longshot wind tunnel- its measurement and evaluation" VKI TN 98, 1974.

9. ERIKSEN L. and GOLDSTEIN R.J. : "Heat transfer and film cooling following injection through inclined circular tubes" J. of Heat Transfer, Transactions of ASME, Vol. 96, Series C, N°2, May 1974. pp.239-245.

10. BLAIR M.F. : "An experimental study of heat transfer on film-cooling on large-scale turbine endwalls" ASME PAPER 74-GT-33, April 1974.

11. WHITNEY W.J.; SCANZA E.M., MOFFIT T.P., and MARVOE D.E. : "Cold air investigation of a turbine for a high temperature engine application-part 1." NASA TN D 3751, January 1967.

12. VAN DEN BRAEMBUSSCHE R.A. : "Calculation of compressible subsonic flow in cascades with varying blade height" ASME PAPER 73-GT-59, April 1973.

13. SPALDING D.B. and CHI S.W. : "The drag of a compressible
    turbulent boundary layer on a smooth flat plate with
    and without heat transfer"
    J. of Fluid Mechanics, Vol. 18, part 1, January 1964.

14. CONSIGNY H., RICHARDS B.E., and VILLE J.P. : "Short duration
    measurements of heating to cooled gas turbine surfaces"
    ASME PAPER 78-GT-22, April 1978.

15. DODGE P.R. : "Numerical method for 2D and 3D viscous flows"
    AIAA Journal, Vol. 15, N°15, July 1977.

16. HORLOCK J.H. : "Secondary flows"
    VKI LS 72, January 1975.

17. KENNY D.P. : "A method for calculating cascade channel endwall
    boundary layer crossflow"
    ASME PAPER 76-GT-77, April 1976.
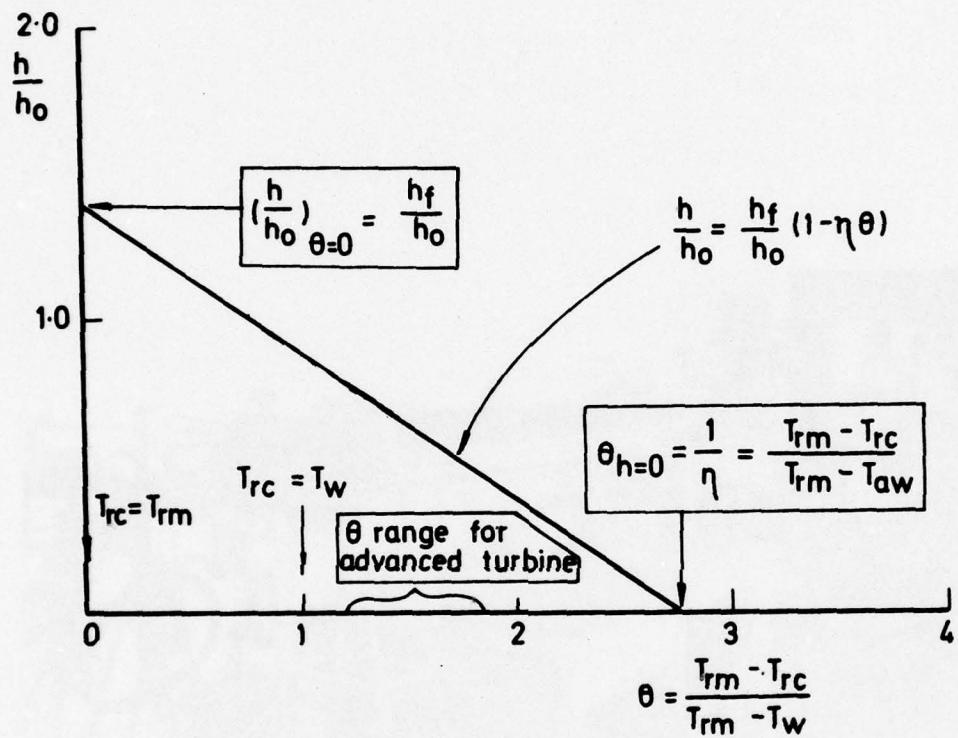
FIG. 1 VARIATION OF HEAT TRANSFER COEFFICIENT, h
WITH THE COOLANT TEMPERATURE PARAMETER, θ
FOR GIVEN EXTERNAL FLOW CONDITION, x , m AND
HOLE GEOMETRY.
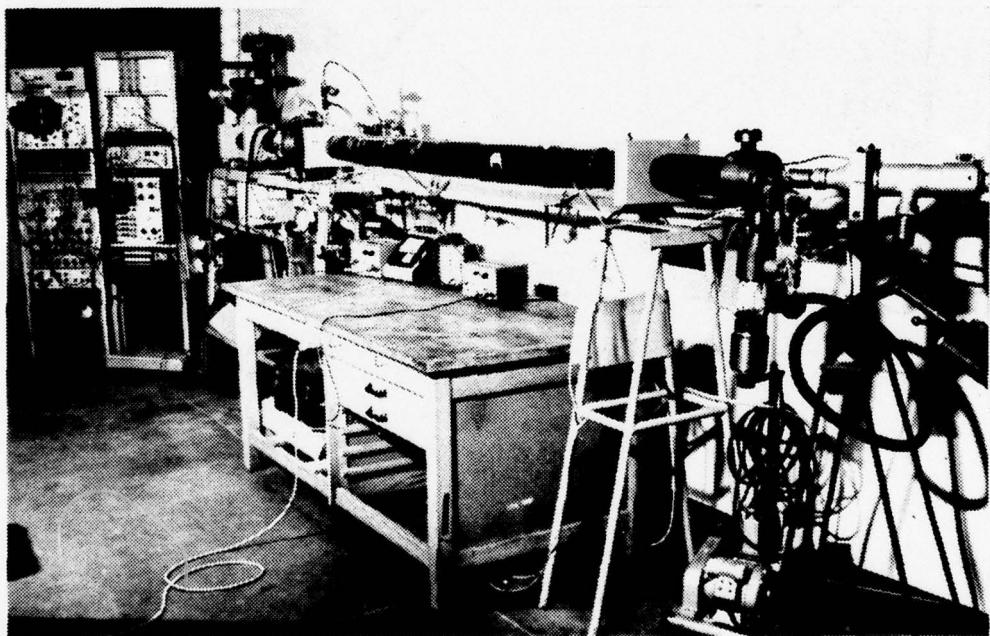
FIG. 2   THE CT1 FACILITY
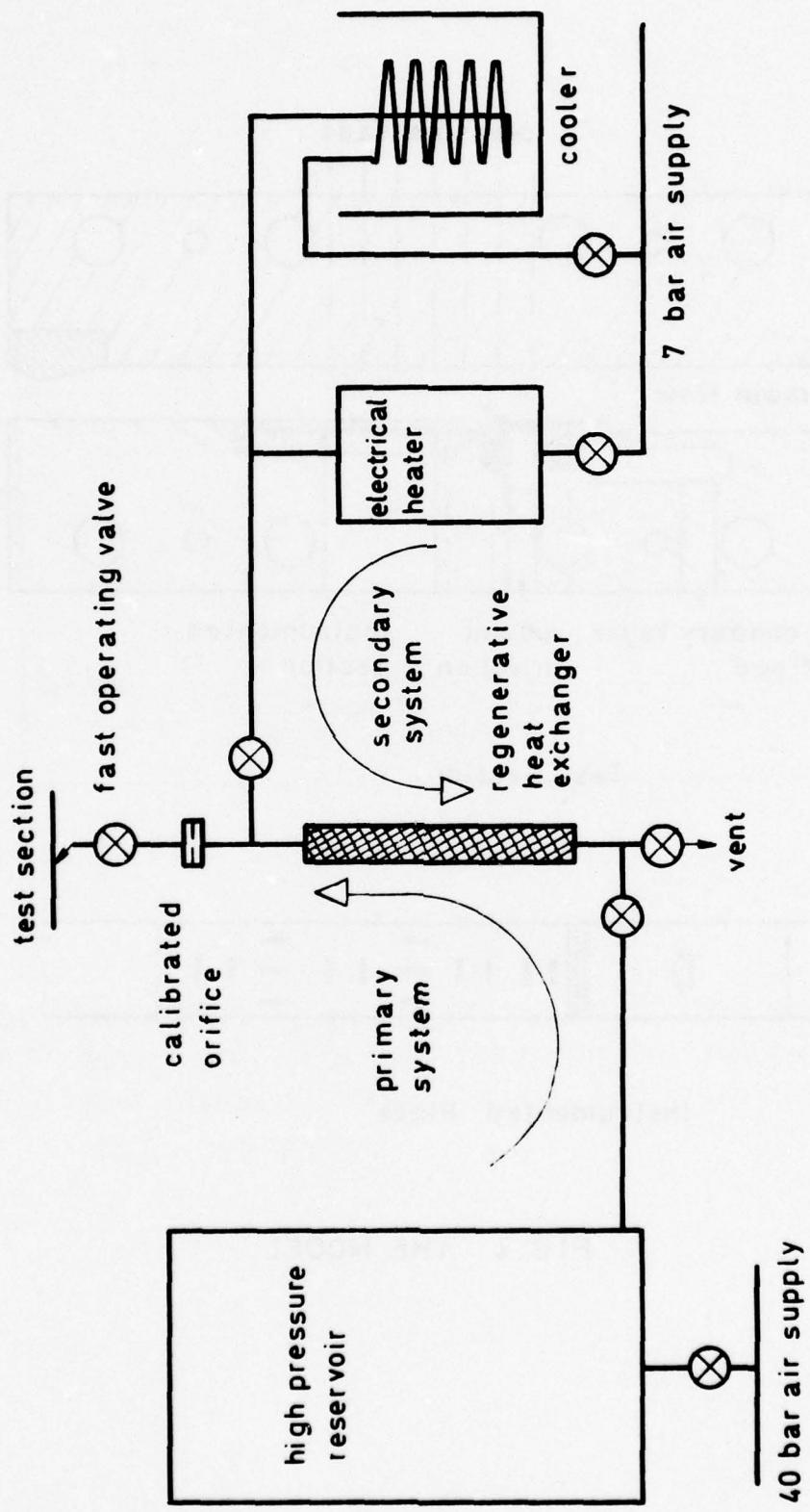
FIG. 3   SECONDARY GAS AIR SUPPLY

pressure taps

main flow

boundary layer   coolant   instrumented
bleed   injection   section
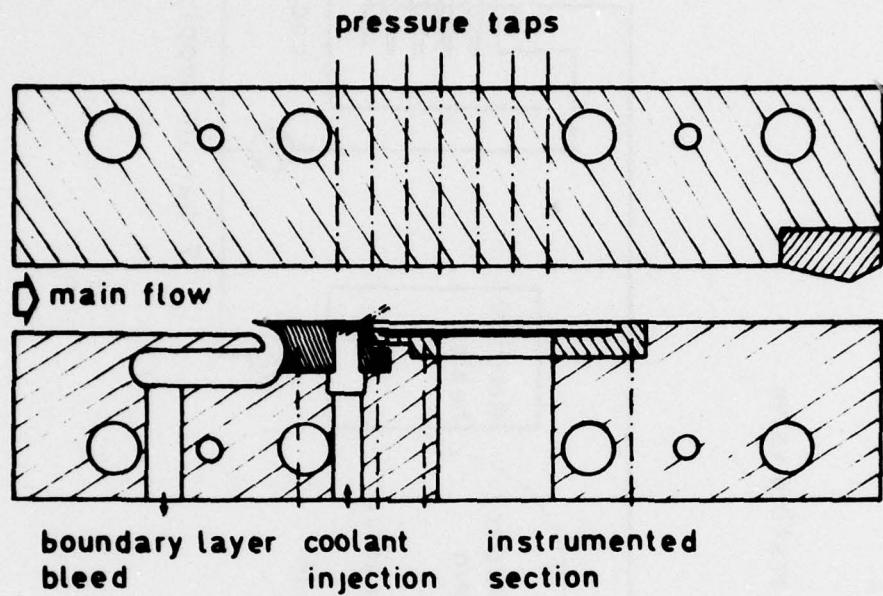
Test Section
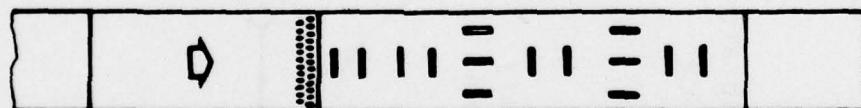
Instrumented Plate

FIG. 4   THE MODEL
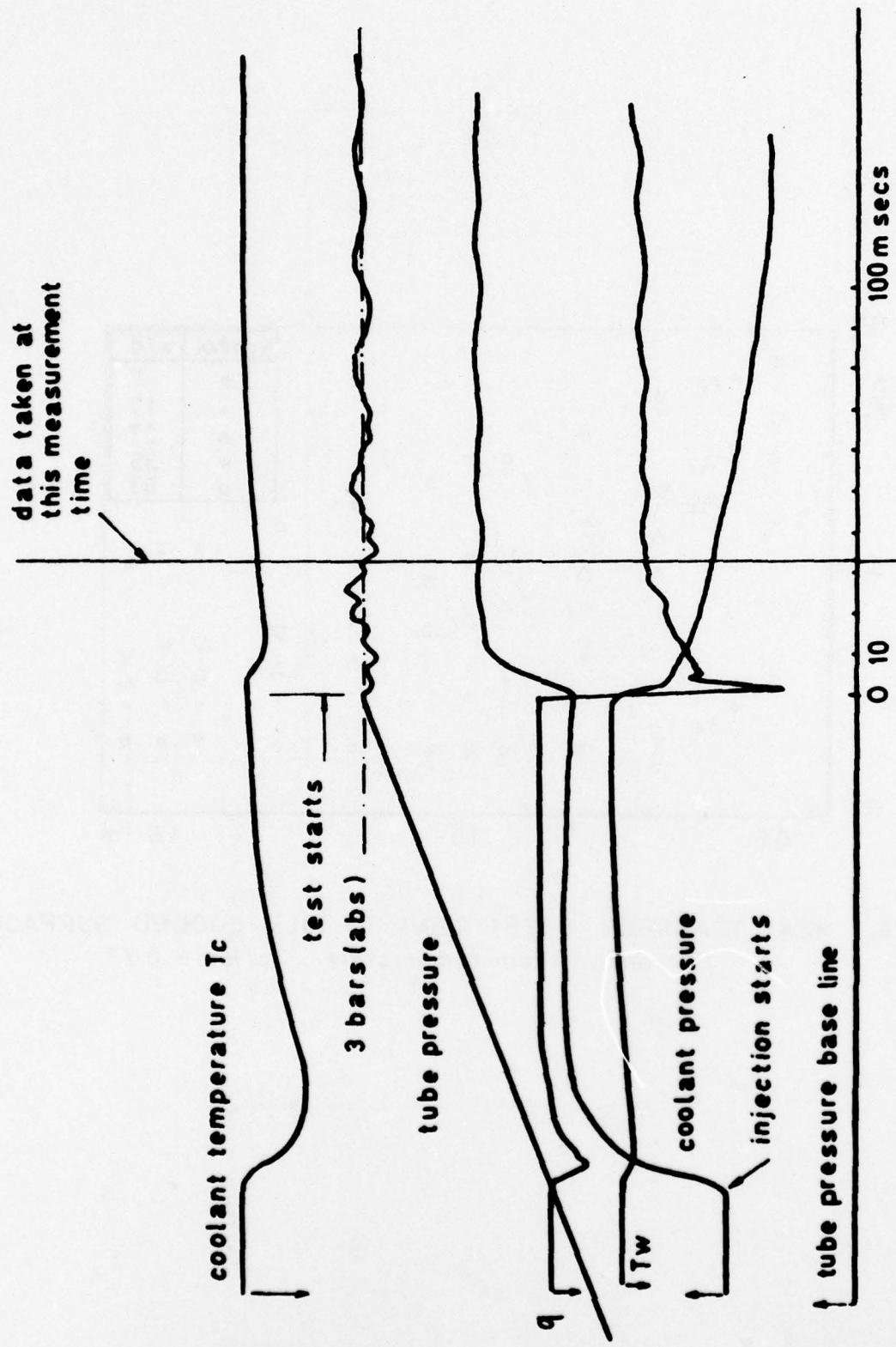
FIG. 5 TYPICAL TRACES OBTAINED (FILM AT ROOM TEMPERATURE)
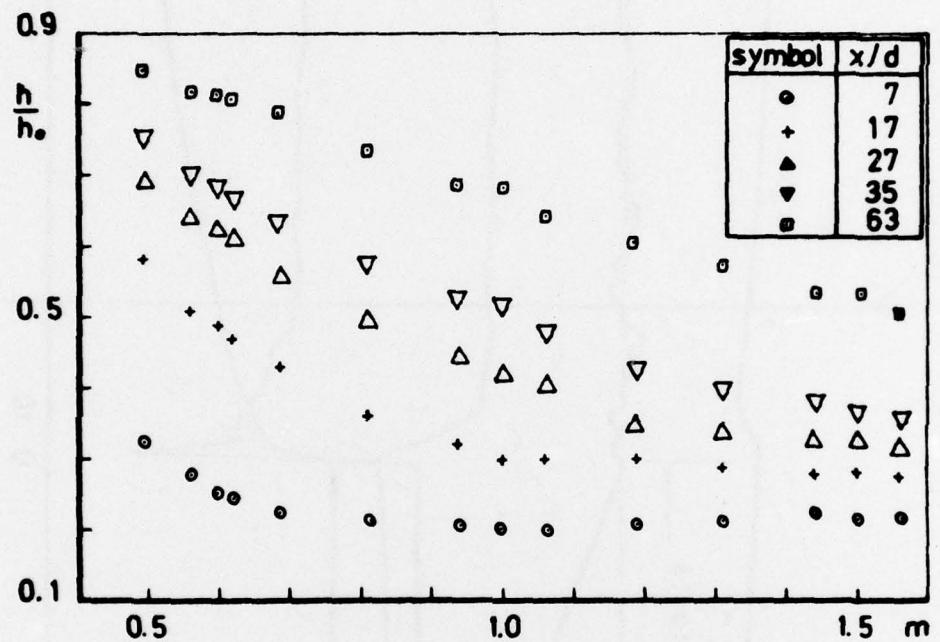
FIG. 6   HEAT TRANSFER COEFFICIENT TO FILM COOLED SURFACES
Coolant at room temperature   Tc/Tom = 0.77
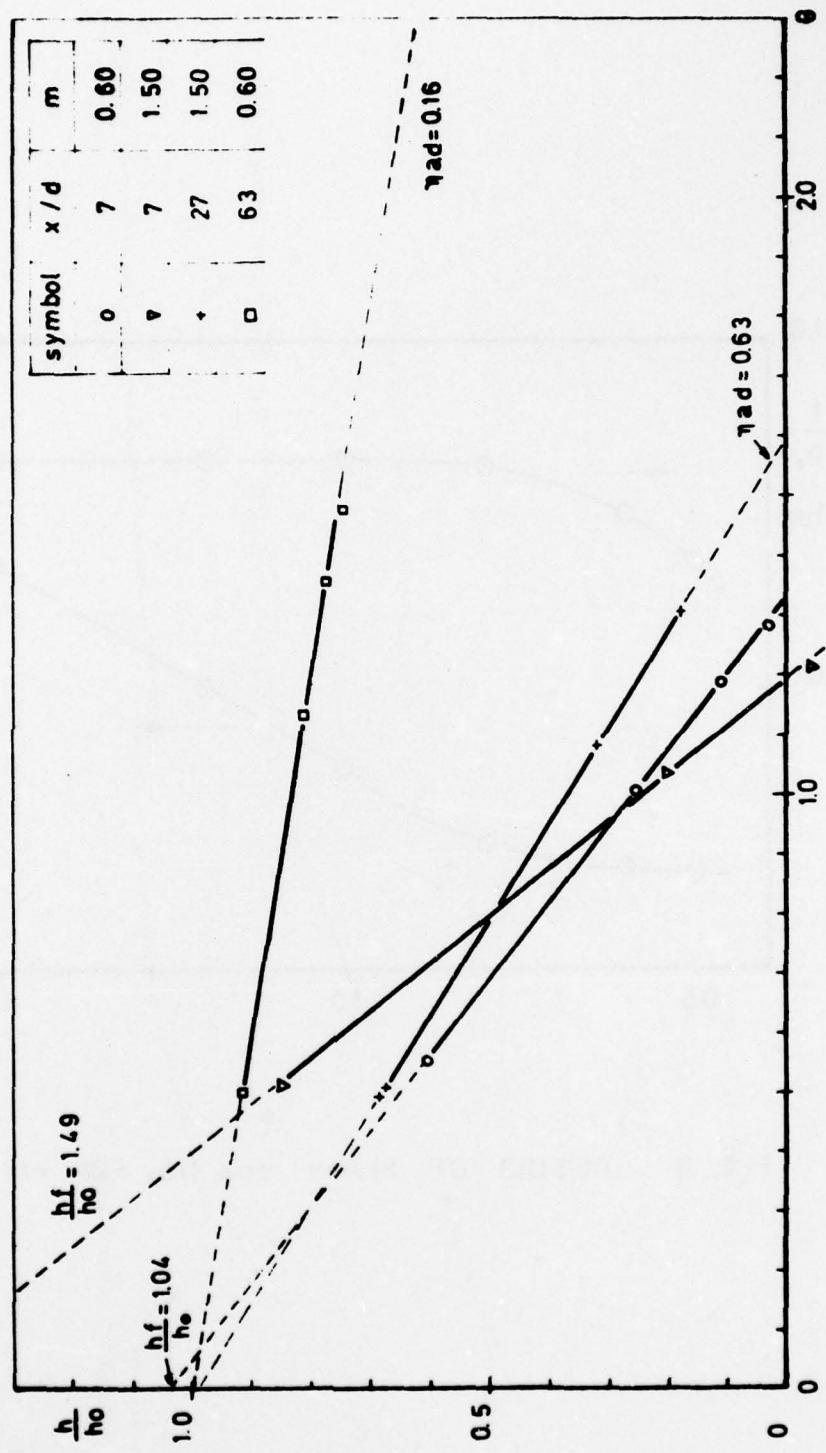
FIG.7 TYPICAL VARIATIONS OF HEAT TRANSFER COEFFICIENT WITH TEMPERATURE PARAMETER θ

symbol	x / d	m
o	7	0.60
▲	7	1.50
+	27	1.50
□	63	0.60

$\eta ad=0.16$

$\eta ad=0.63$

$\dfrac{hf}{ho}=1.49$

$\dfrac{hf}{ho}=1.04$

$\dfrac{h}{ho}$

1.0

0.5

0

0

1.0

2.0

θ
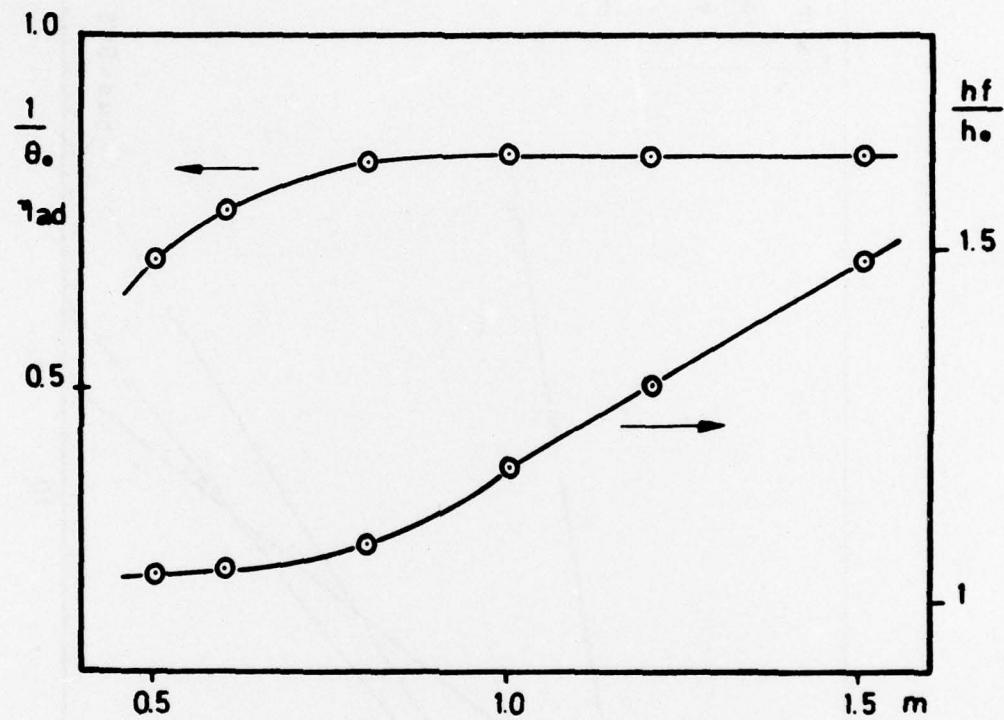
FIG. 8   RESULT OF hf/ho and 1/θ. FOR x/d = 7
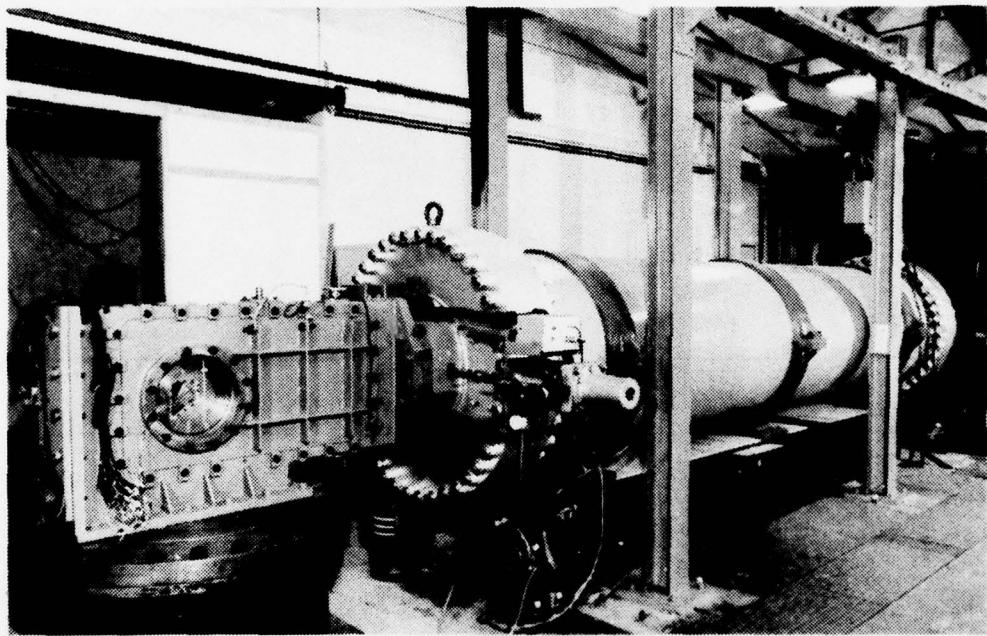
FIG. 9. THE CT 2 HOT CASCADE FACILITY

turbine nozzle blade   (ref. 13)
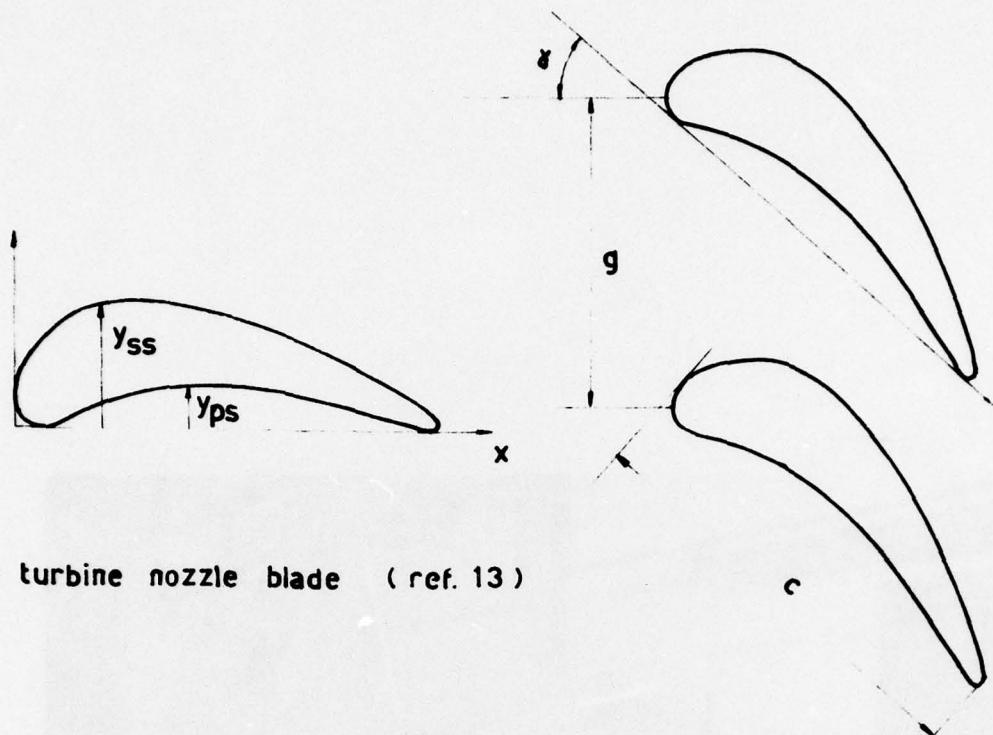
| x/c	y_{ps}/c	y_{ss}/c	x/c	y_{ps}/c	y_{ss}/c	x/c	y_{ps}/c	y_{ss}/c
0.000	.068	.068	.363	.097	.288	.728	.070	.178
.045	—	.170	.410	.103	.282	.773	.058	.157
.092	—	.222	.455	.105	.270	.820	.047	.135
.137	.027	.253	.500	.103	.260	.865	.033	.110
.182	.048	.275	.547	.102	.247	.910	.022	.083
.228	.065	.287	.592	.097	.232	.957	.007	.055
.273	.080	.293	.637	.090	.215	1.000	.017	.017
.318	.090	.293	.683	.080	.197			

FIG.10   BLADE   COORDINATES AND CASCADE GEOMETRY
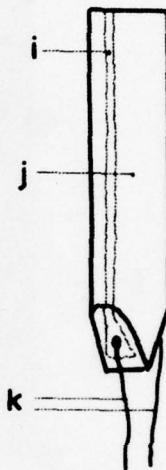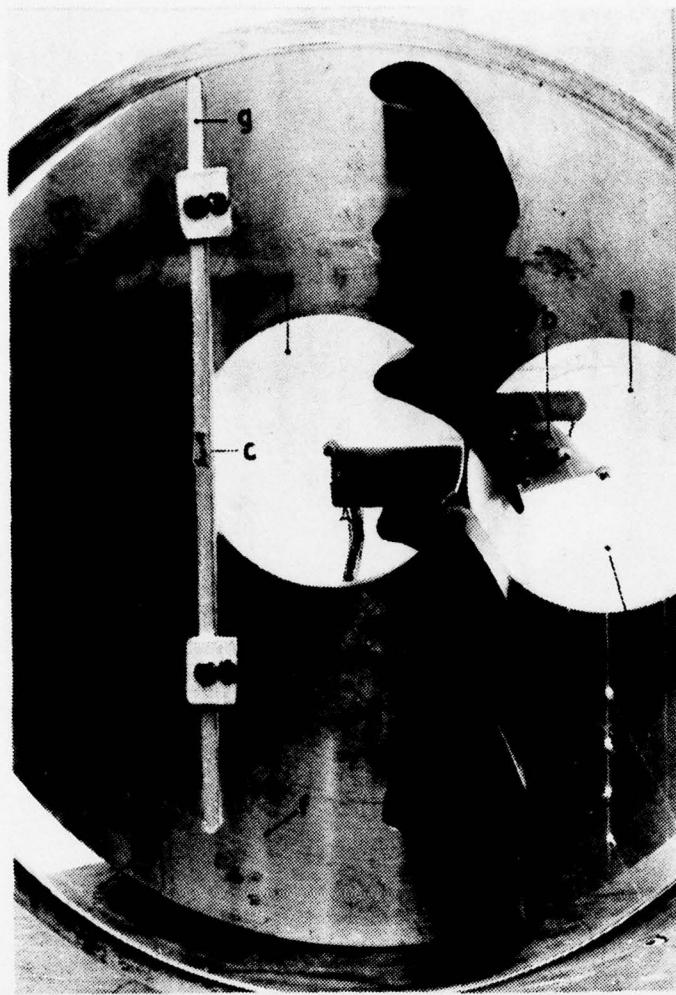
a   rotating   pieces (perspex)

b   heat transfer gauge

c-d   inlet and outlet static pressure holes

e   perspex window opposed to the measurement zone

f steel window supporting the rotating pieces

g aluminium wedge fixed in the perspex window

h platinum   thin film

i silver connections

j pyrex rod

k soldered wires

FIG.11   GENERAL   VIEW   OF   THE   MODEL
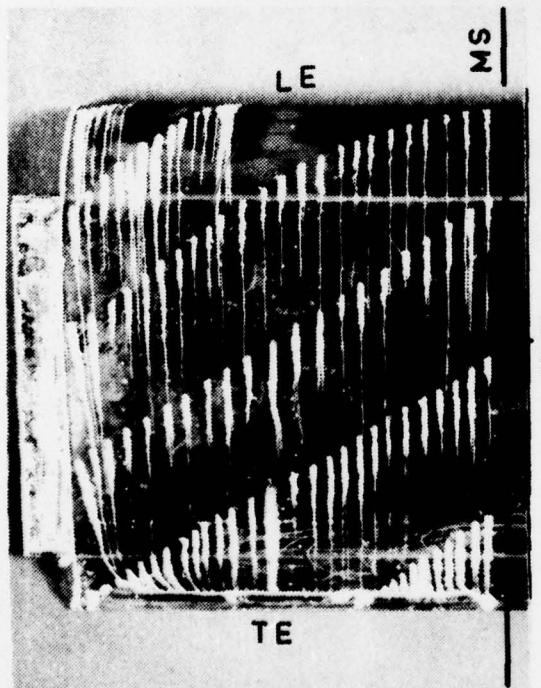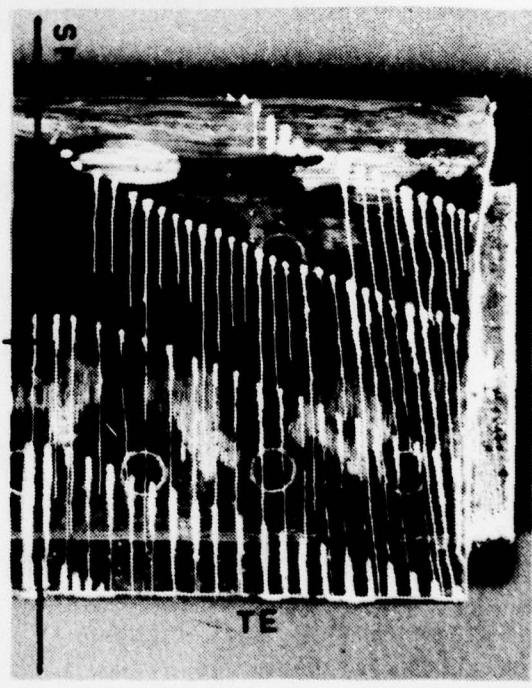
suction side   pressure side

FIG.12   OIL   DROPS   VISUALIZATION   RESULT

1.7

2.2

2.6

1.7

1.9

3.1

2.1

3.0

3.4

3.5

q (W/cm^2)

4.1

2.9

1.7   2.8

3.6

2.6

4.8

$M_1 = 0.24$

$p_{01} = 1.83$ bar

$T_{01} = 390$ K
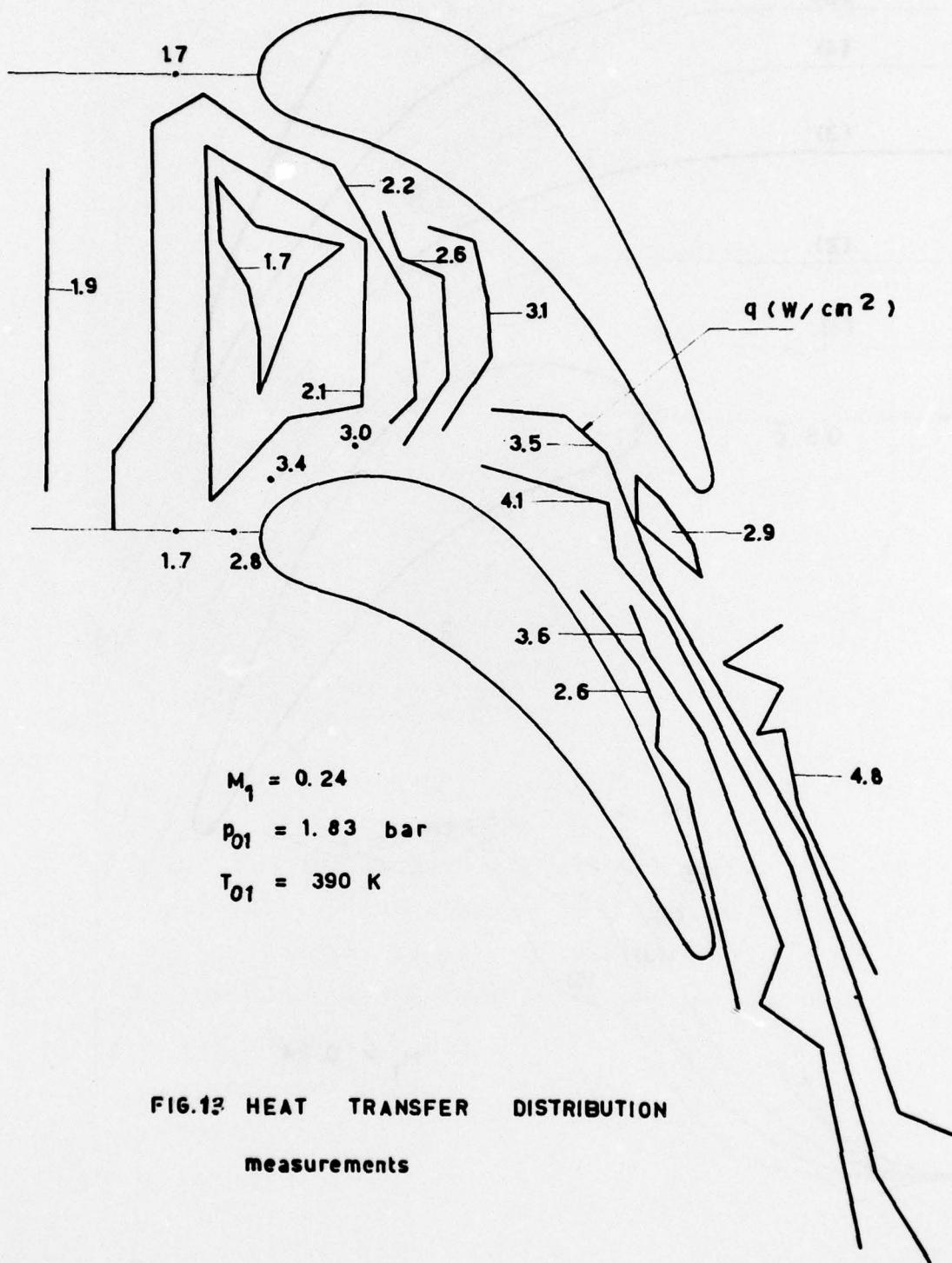
FIG.13 HEAT TRANSFER DISTRIBUTION

measurements

$M_1 = 0.24$
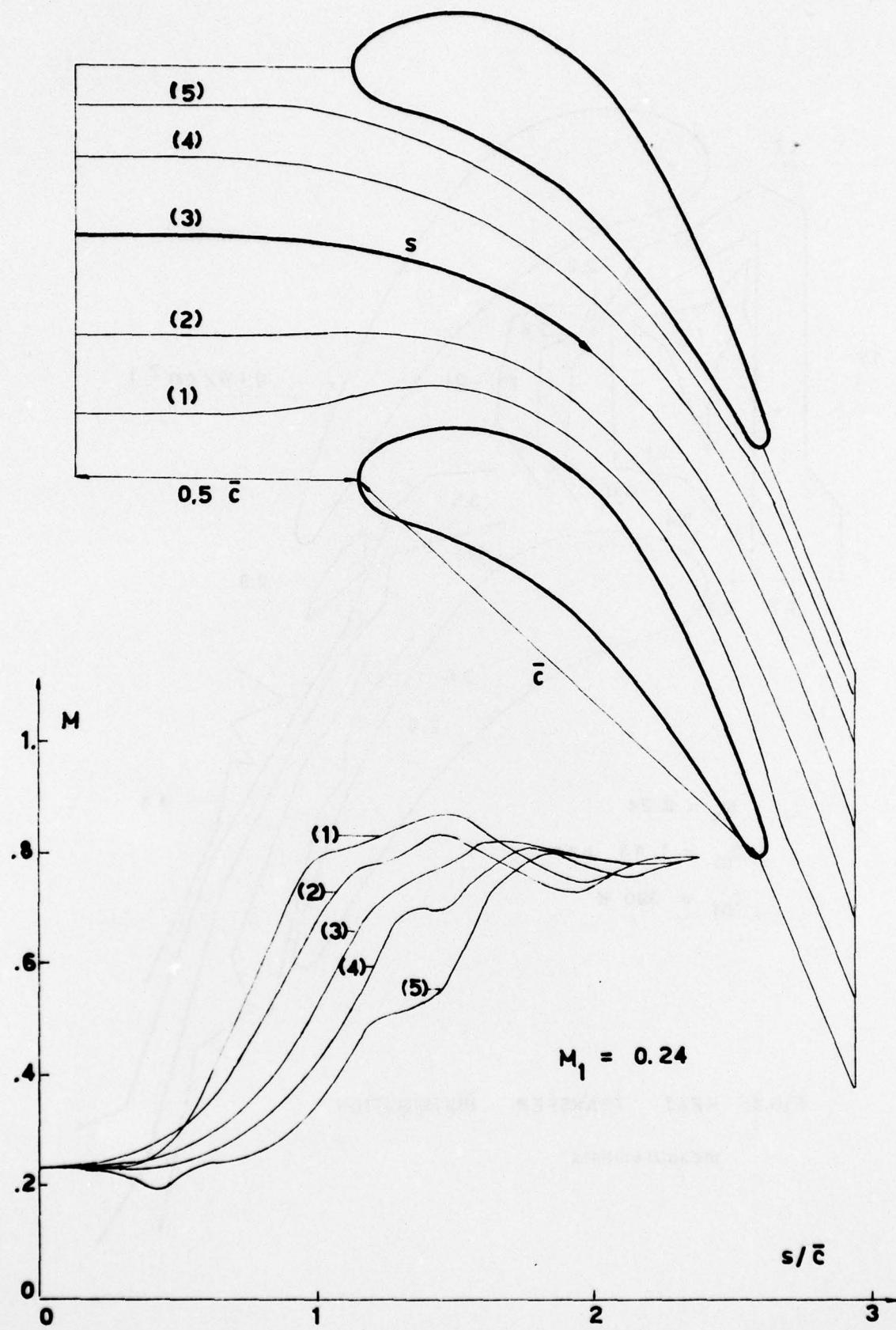
FIG.14 2D STREAMLINES AND CALCULATED MACH NUMBERS
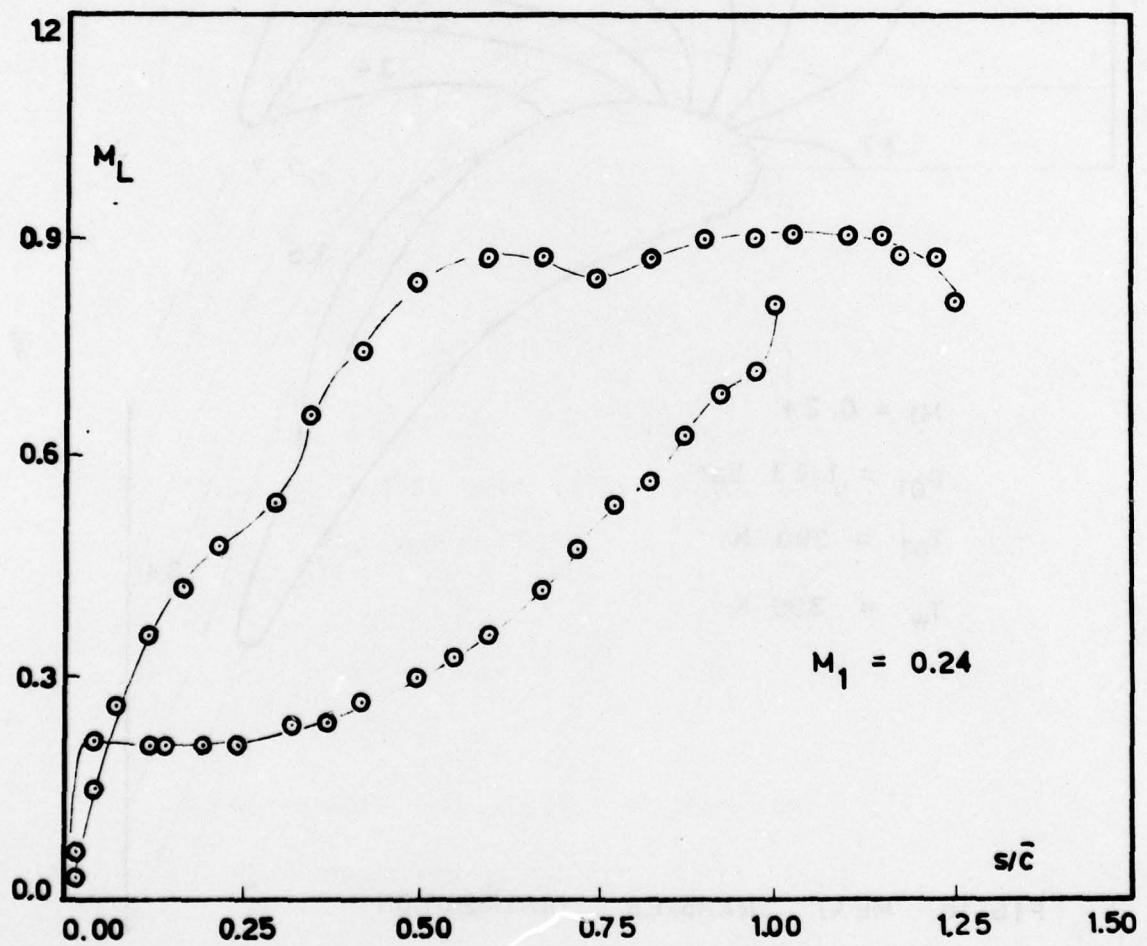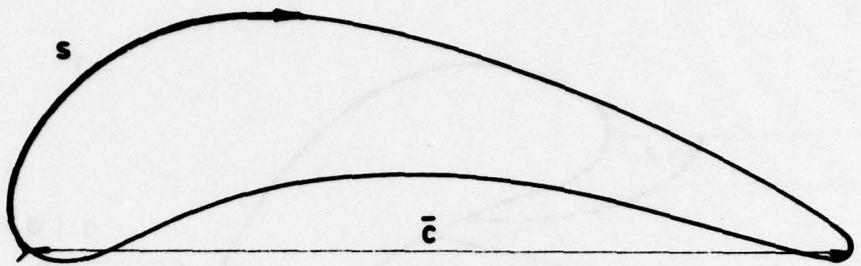
FIG.15 BLADE – SURFACE MACH NUMBER
DISTRIBUTION

$q \ (W/cm^2)$

1.9   1.9   2.1   2.3   2.6   3.0   3.2   3.4   3.5   3.4   1.7   1.7

$M_1 = 0.24$

$P_{01} = 1.83 \ bar$

$T_{01} = 390 \ K$

$T_W = 309 \ K$
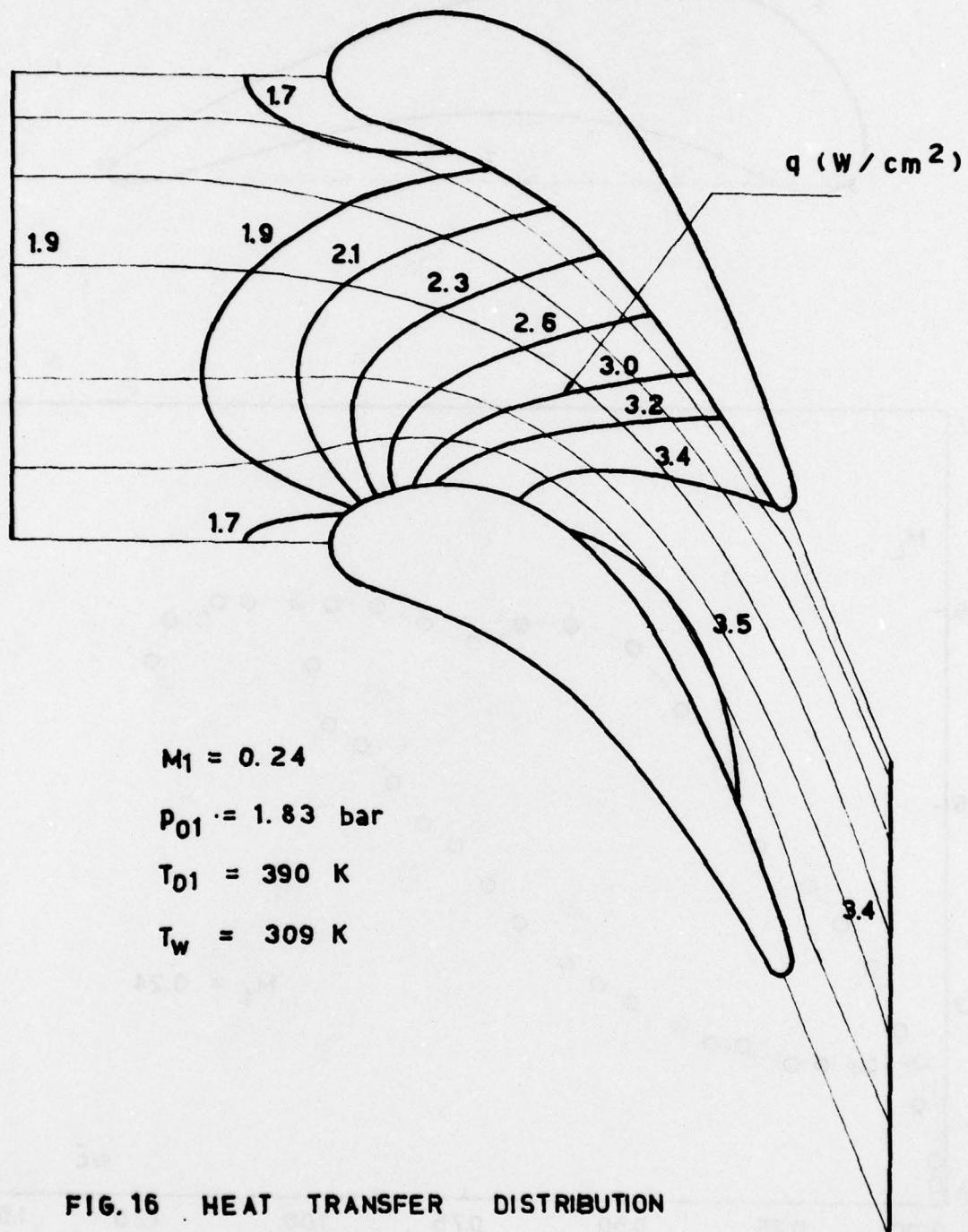
FIG. 16   HEAT   TRANSFER   DISTRIBUTION
calculation

REPORT DOCUMENTATION PAGE		READ INSTRUCTIONS BEFORE COMPLETING FORM
1. REPORT NUMBER	2. GOVT ACCESSION NO.	3. RECIPIENT'S CATALOG NUMBER
4. TITLE (and Subtitle) FILM COOLING AND END WALL HEAT TRANSFER IN SMALL TURBINE BLADE PASSAGES		5. TYPE OF REPORT & PERIOD COVERED 2nd year annual report July 76 - Dec 77
		6. PERFORMING ORG. REPORT NUMBER
7. AUTHOR(s) VILLE, J-P; GODARD, M.; RICHARDS, B.E.; SIEVERDING, C.		8. CONTRACT OR GRANT NUMBER(s) DA-ERO-75-074
9. PERFORMING ORGANIZATION NAME AND ADDRESS von Karman Institute for Fluid Dynamics Chaussée de Waterloo, 72 B-1640 Rhode Saint Genèse, Belgium		10. PROGRAM ELEMENT, PROJECT, TASK AREA & WORK UNIT NUMBERS 61102A-1T161102B35E-00-530
11. CONTROLLING OFFICE NAME AND ADDRESS		12. REPORT DATE February 1978
		13. NUMBER OF PAGES 47
14. MONITORING AGENCY NAME & ADDRESS(if different from Controlling Office) USA R&S GP (EUR) Box 65 FPO New York 09510		15. SECURITY CLASS. (of this report) UNCLASSIFIED
		15a. DECLASSIFICATION/DOWNGRADING SCHEDULE

16. DISTRIBUTION STATEMENT (of this Report)

Approved for public release
Distribution unlimited

17. DISTRIBUTION STATEMENT (of the abstract entered in Block 20, if different from Report)

18. SUPPLEMENTARY NOTES

19. KEY WORDS (Continue on reverse side if necessary and identify by block number)

Propulsion, internal flows, film cooling, cascade flows

20. ABSTRACT (Continue on reverse side if necessary and identify by block number)

Two topics have been studied related to the cooling of the end wall of a turbine passage. The first concerns the development of a method for measuring the adiabatic wall effectiveness and heat transfer coefficient of a film cooling system for protecting a surface from high heating derived from a hot compressible flow. The second concerns the measurement of the heat transfer rate distribution to a turbine cascade end wall in order to choose an appropriate film cooling system. These are related to providing the background to the final phase of the study in which the effectiveness of a film cooling system to cool a turbine end wall will

DD FORM 1473   EDITION OF 1 NOV 65 IS OBSOLETE

Abstract (con'd)
be made, combined with the measurement of the aerodynamic losses incurred by
such a system.